ELSEVIER

Coordination Chemistry Reviews 237 (2003) 53–63

COORDINATION CHEMISTRY REVIEWS

www.elsevier.com/locate/ccr

The medicinal and catalytic potential of model complexes of vanadate-dependent haloperoxidases

Dieter Rehder [a,*], Gabriella Santoni [a], Giulia M. Licini [b], Carola Schulzke [c], Beate Meier [d]

[a] *Institut für Anorganische und Angewandte Chemie, Universität Hamburg, Martin-Luther-King-platz 6, D-20146 Hamburg, Germany*
[b] *Dipartimento di Chimica Organica, Universitá degli Studi di Padova, I-35131 Padova, Italy*
[c] *Institut für Anorganische Chemie, Universität Kiel, 24098 Kiel, Germany*
[d] *bcm-Research Institute, D-85307 Entrischenbrunn, Germany*

Received 25 January 2002; accepted 16 October 2002

Contents

Abstract

Vanadium(V) complexes predominantly of composition VO(O_3N), modeling the active center of vanadate-dependent haloperoxidases, are investigated with respect to (i) their catalytic potential in enantio-selective oxidation by peroxide of prochiral sulfides, and (ii) their in vitro cytotoxicity and insulin-mimetic ability towards fibroblast cell cultures. The peroxidation of methyl-tolylsulfide with cumyl-hydroperoxide, which is related to the sulfideperoxidase activity of haloperoxidases, is catalyzed by (*RRR*)-[VO(OMe)L] [H_2L = (*R*,*R*)-bis(2-phenylethanol)-(*R*)-1-phenylethylamine] as well as by a mixture of [VO(O*i*Pr)$_3$] and H_2L to an enantiomeric excess (ee) of 25%. The crystal and molecular structures of (*RRR*)-[VO(OMe)L] · 1/2MeOH are reported. In the context of the phosphatase activity of the apo-haloperoxidases, possible modes of action of vanadium compounds in insulin-mimesis are addressed. In vitro results for seven oxovanadium(IV) and -(V) coordination compounds show that, at essentially non-toxic concentrations [c(V) < 0.1 mM], the compounds trigger glucose intake into human and simian virus modified mice fibroblasts, in several cases at a higher level than insulin.

Keywords: Haloperoxidase; Sulfide oxidation; Vanadium complexes; Insulin-mimesis

* Corresponding author
E-mail address: dieter.rehder@chemie.uni-hamburg.de (D. Rehder).

0010-8545/02/$ - see front matter
PII: S0010-8545(02)00300-4

1. Introduction

The three vanadate-dependent peroxidases which have so far been structurally characterized all show a high degree of amino acid sequence homology in their active centers and thus almost identical active site structures (Fig. 1a), irrespective of their origin from brown algae (*Ascophyllum nodosum*, *A.n.*) [1], red algae (*Corallina officinalis*, *Co.o.*) [2] or fungi (*Curvularia inaequalis*, *Cu.i.*) [3]. Vanadate is covalently linked to the Nε of an imidazolyl moiety of a proximal histidine, and is further in hydrogen bonding contact, via an axial OH group, to a distal ('catalytic') histidine and water molecules. The overall geometry is trigonal–bipyramidal. On coordination of peroxide, structural rearrangement occurs in that the axial (proximal) His moves into a basal position, giving rise to a tetragonal {$VO(O_2)OH(His)$} pyramid with the peroxo ligand occupying two equatorial positions in the symmetrical side-on manner (Fig. 1b) common for peroxovanadium complexes [4]. This peroxo form has been structurally characterized for the fungal *Cu.i.* enzyme [5]. For solutions of the *A.n.* peroxidase treated with ^{17}O enriched H_2O_2 it has been proposed on the basis of ^{17}O-NMR that asymmetrically side-on coordinated hydroperoxide (Fig. 1c) is also present [6], providing a site for nucleophilic attack of a substrate to be oxidized, such as halide or organic sulfide. We have recently modeled a situation which comes close to a hydroperoxovanadium complex, viz. $[VO(O_2)bpah] \cdot 2H_2O$ (bpha = *NN*-bis(2-pyridylmethyl)-β-alanine) where, in a supramolecular arrangement, a water of crystallization is hydrogen-linked to one of the oxygens of the peroxo ligand [7] (Fig. 1d). The following reactions (eqns. 1 and 2) have been noted for vanadate-dependent haloperoxidases:

$$Hal^- + H_2O_2 + H^+ \rightarrow HalOH + H_2O \quad (Hal = \text{halide},\ SCN^-) \qquad (1)$$

followed by the non-enzymatic step $RH + HalOH \rightarrow RHal + H_2O$.

$$RSR' + H_2O_2 \rightarrow RS(O)R' + H_2O \qquad (2)$$

Enantioselective sulfoxidations with the enzyme [8] are of interest in the light of the availability of chiral auxiliaries in asymmetric syntheses [9]. An additional intrinsic feature of haloperoxidases is their phosphatase activity after removal of vanadate [10]. Reconstitution of the apoenzyme with vanadate restores the peroxidase activity at the expense of the phosphatase activity, an observation which goes along with the well established ability of vanadate to inhibit phosphatases [11]. Quite interestingly, the peroxidases of *A.n.*, *Co.o.* and *Cu.i.* all contain the same structural motif of an acid phosphatase from *Escherichia blattae*, which has recently been structurally characterized [12]. In addition, there is very close sequence homology between the active sites of this phosphatase and all three haloperoxidases, which fact may hint towards a common phylogenetic origin or convergent evolution. It has been proposed (for details see Section 2.2) that inhibition of a protein–tyrosine–phosphatase can be the key step in insulin-mimetic actions of vanadium compounds.

2. Results and discussion

2.1. Sulfoxidation

Specific vanadium Schiff-base complexes, or mixtures of the constituents thereof, can be employed in the catalytic oxidation of sulfides (thioethers) to sulfoxides and further to sulfones, using H_2O_2 or organic hydroperoxides [13–16]. If prochiral sulfides are used, chiral sulfoxides are generated. In order to match the vanadium environment {$VO(O_3N)$} at the active site of the vanadate-dependent peroxidases, we have employed tridentate aminoalcohols $(HO)_2N$, H_2L, as ligands (**1** in Scheme 1) which, when reacted with appropriate vanadium precursor compounds such as $[VO(OiPr)_3]$ in methanol, lead to vanadium(V) complexes of composition [VO(OMe)L] (**2** in Scheme 1). The ligands resemble those which have previously been successfully employed in enantioselective sulfoxidations with titanium(IV)- and zirconium(IV)-based catalysts [17,18]. The chiral ami-

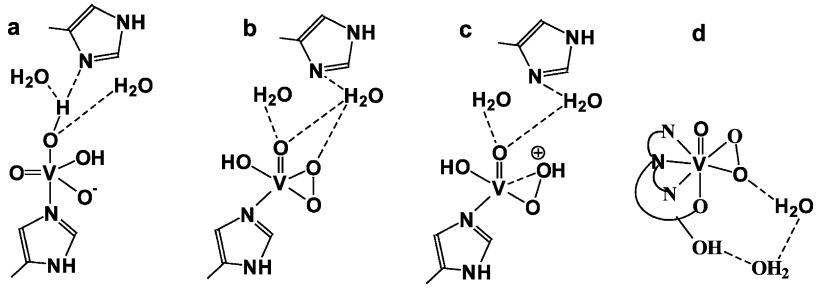

Fig. 1. Active site structures of the algal and fungal haloperoxidases (a) and of the peroxo form of the fungal peroxidase from *C. inaequalis* (b). Also shown are the assumed formation of a hydroperoxo intermediate (c), and a model compound with a frozen-in switch-on–switch-off state for delivery of a proton to a coordinated peroxo group (d).

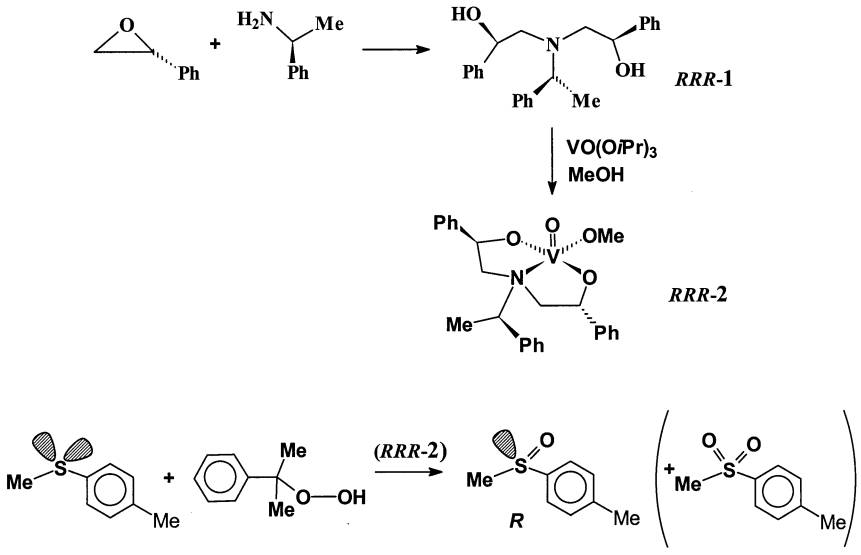

Scheme 1.

noalcohols can be obtained from the ring-opening reaction between amines and enantiopure epoxides.

The structure of complex **2** has been solved by X-ray diffraction analysis. A SCHAKAL plot and numbering scheme is given in Fig. 2, selected bonding parameters in Table 1, crystal data and structure refinement in Table 2. The complex attains a strongly distorted tetragonal bipyramid with the oxo group in the apex. Vanadium is displaced from the plane spanned by the four ligand functions by 0.52 Å. V–O bond lengths and bond angles are in the expected range. The amine-N is in *trans* position to the methoxy group (the angle N–V–O4 is 167.77(7)°); the V–N bond, 2.2906(18) Å, is substantially elongated with respect to a common V–N single bond, although not to the extent as in complexes where the nitrogen function is *trans* to an oxo group (2.5–2.6 Å [16,19a]). In solutions of $CDCl_3$, two resonance signals of about equal intensity arise at −414 and −457. The shift difference is too large as to account for diastereomers arising from enantiomers [19b]; we can thus exclude chiral interconversion in solution. A possible explanation for the presence of two isomers is a structural rearrangement, leading to an equilibrium between a tetragonal–pyramidal complex and a

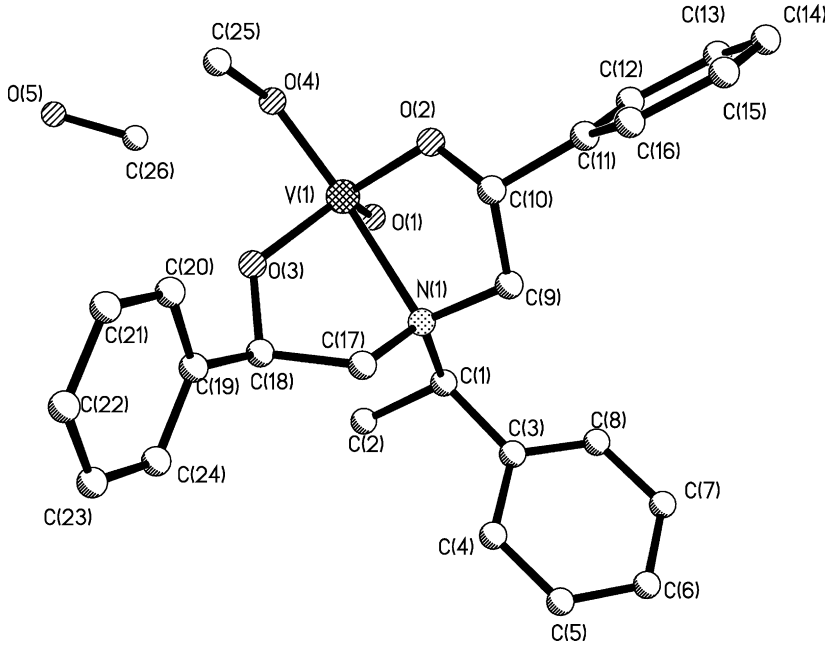

Fig. 2. SCHAKAL plot and numbering scheme for complex **2**, including MeOH.

Table 1
Selected bond lengths (Å) and bond angles (°) for **2**

Bond lengths	
V–O1	1.5933(15)
V–O2	1.8023(13)
V–O3	1.8092(16)
V–O4	1.7921(15)
V–N1	2.2906(18)
N1–C1	1.523(3)
N1–C9	1.479(2)
N1–C17	1.480(3)
Bond angles	
O1–V–O2	113.76(8)
O1–V–O3	118.87(8)
O1–V–O4	102.70(7)
O1–V–N1	89.24(7)
O2–V–O4	97.80(8)
O2–V–N1	79.44(7)
O3–V–O4	93.20(7)
O3–V–N1	78.51(7)

Table 2
Crystal data and structure refinement for **2** · 1/2MeOH

Emperical formula	$C_{25.5}H_{30}NO_{4.5}V$
Molecular mass (g mol^{-1})	473.45
Crystal system/space group	Monoclinic/*C*2
Unit cell dimensions	
a (Å)	16.5663(14)
b (Å)	9.7046(8)
c (Å)	15.4080(13)
β (°)	105.7060(10)
Volume (Å^3); *Z*	2384.6(3); 4
Calculated density (g cm^{-3})	1.319
Absorption coefficient (mm^{-1})	0.449
F(000)	996
Crystal size (mm)	0.6 × 0.2 × 0.1
θ Range (°)	2.46–27.55
Limiting indices	$-21 < h < 21$; $-12 < k < 12$; $-20 < l < 19$
Reflections collected	14 215
Unique reflections	5351
R_{int}	0.0415
Refined parameters	300
Goodness-of-fit on F^2	0.832
Final R_1 [$I > 2\sigma(I_0)$]	0.0392
Final R_2 [$I > 2\sigma(I_0)$]	0.0519
R_1 (all data)	0.0594
R_2 (all data)	0.0554
Absolute structural parameter	0.004(16)
Differential peak and whole (e Å^{-3})	0.812 and −0.442

trigonal–bipyramidal species, presumably with the amine function in one of the apical positions as in the active center of the enzyme, or in structurally characterized octahedral aminoalcoholato–vanadium complexes such as [VO(acac)L′] [H_2L' = diethanol-*R*/*S*-1-phenylethylamine] with a very weak V···N bond [16,19a].

The catalytic potential in sulfide oxidation was studied in detail with authentic **2** on the one hand, and mixtures of **1** and [VO(O*i*Pr)$_3$] on the other hand. Methyl-tolylsulfide and cumyl-hydroperoxide were employed at concentrations of 0.1 M, the catalyst system at 0.01 M in anhydrous dichloromethane solution. The reaction (cf. Scheme 1) yields the sulfoxide as the main component along with minor amounts of the sulfone. The results are presented graphically in Fig. 3.

Catalyst **2** (*RRR*-configuration) leads to an about 90% oxidation of the sulfide within 2 h. The main product formed is the *R* isomer of the sulfoxide. The enantiomeric excess (ee) in this reaction amounts to 25%, remaining constant during the complete reaction period. The same product spectrum, both with respect to the ratio of sulfoxide and sulfone, and the ee, is obtained as a mixture of ligand **1** (*RRR*-configuration) and precursor [VO(O*i*Pr)$_3$] is used as the catalyst, pointing towards the same intermediate in oxidation catalysis. This assumption is corroborated by comparable features in the ^{51}V-NMR spectra of (i) [VO(O*i*Pr)$_3$]+**1**+the organic peroxide and (ii) complex **2**+organic peroxide: in either case, a distinct signal arises at $\delta(^{51}V) = -510$ on addition of the peroxide, very possibly accounting for a peroxo complex of composition [VO(OOR)L]. There is, however, also an apparent difference in the two catalyst systems: in the case of a mixture of **1** and [VO(O*i*Pr)$_3$], the reaction proceeds sufficiently faster (by a factor of 5). The reason for this accelerating effect (or decelerating effect with respect to complex **2**) is unclear.

Reaction times, yields and ee in vanadium catalyzed sulfoxidations of arylsulfides largely depend on the nature of substituents on the phenyl ring. Reaction times with our catalysts are usually shorter than in other reported systems, while yields are comparable or better. Examples from the literature are the oxidation of arylalkylsulfides with H_2O_2 catalyzed by [VO(acac)$_2$] in the presence of Schiff bases based on chiral aminomonoalcohols and salicylaldehydes (around 60% yield) [13b], the H_2O_2 oxydation of *p*-tolylmethylsulfide in the presence of *A.n.* peroxidase (18%) [8] or *Co.i.* peroxidase (7%) [20], or the oxidation of *p*-tolylmethylsulfide by cumylperoxide through VO^{2+} complexes with chiral salen related Schiff bases (71%) [15]. The ee in our non-optimized systems are low when compared with the [VO(acac)$_2$]–Schiff base (up to 70%) [13b] and [VO(Schiff base)] systems (35%) [15], and the *A.n.* peroxidase (62%) [8].

2.2. Insulin-mimesis

Insulin influences, among other metabolic pathways, the glucose and the fatty acid metabolism by stimulating glucose uptake by cells, inhibiting glycolysis and glyconeogenesis, and by stimulating lipogenesis. All of these functions have also been reported, from in vitro studies and/or with animal models, for simple inorganic vanadium compounds such as vanadate, peroxovanadate

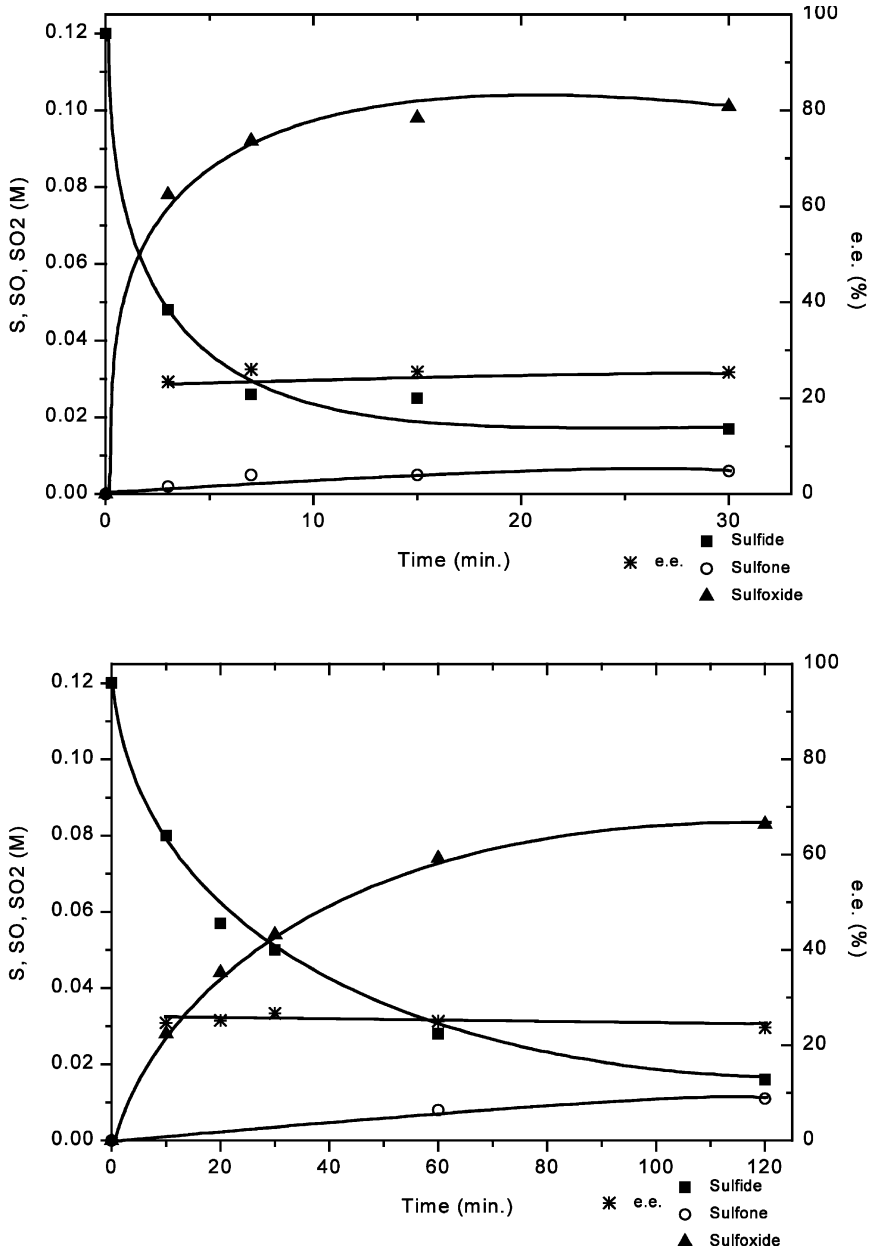

Fig. 3. Change of product pattern and ee with time in the oxidation of methyl-tolylsulfide with cumyl-hydroperoxide in the presence of 10 mol% of **2** (top) or **1**+[VO(O*i*Pr)$_3$] (bottom).

and vanadylsulfate, as well as for more complex vanadium coordination compounds with organic ligands (see refs. [21,22] for a literature overview). Prominent examples for the latter are [VO(ethylmaltolate)$_2$] [23], which just passed clinical tests phase I with diabetic humans, and [NH_4][VO_2(dipicolinate)], which was successfully applied in the treatment of feline patients [24]. Diabetes mellitus may result from lacking insulin production (type 1 diabetes) or from insulin tolerance (type 2 diabetes). Diabetes 2 is the more commonly distributed form. According to the WHO, an estimated 12% of the population in the industrialized countries suffer from diabetes 1 or, more frequently diabetes 2. Cats suffer from type 2 diabetes.

As already mentioned in the Introduction, our link to investigations into the antidiabetic potential of vanadium compounds is the coincident observation that vanadate inhibits phosphatases by binding to or redox-inactivating the phosphatases' active site on the one hand, and the fact that vanadate-dependent peroxidases depleted of vanadate exhibit phosphatase activity on the other hand. The similarity, with respect to sequence homology of the active centers and overall structural features, of certain phosphatases and the peroxidases reflects their comparable affinities for vanadate.

The phosphatases present in the intracellular medium and related to the action of insulin are protein–tyrosine–phosphatases (PTP). The cell membrane con-

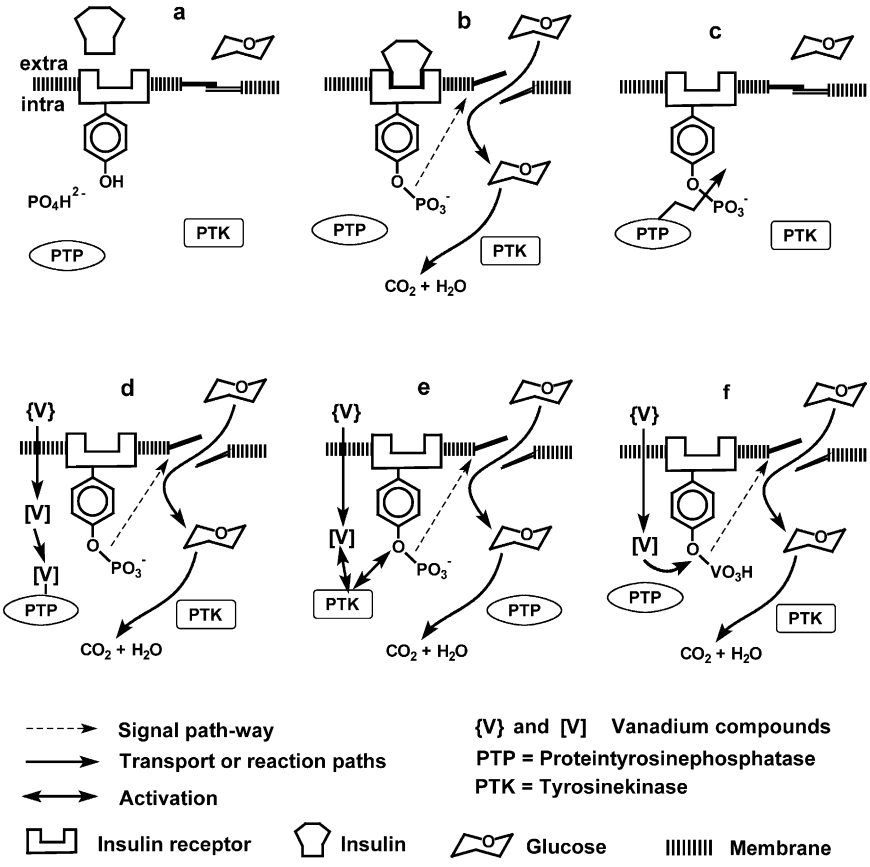

Fig. 4. Schematic representation of the activation of glucose intake by insulin (a, b), blockage of glucose intake in the absence of insulin (c), and the possible counteractions induced by a vanadium compound: (d) inhibition of a phosphatase, (e) activation of a non-membrane kinase, (f) vanadylation of the insulin receptor tyrosine. Details of the signal transduction cascade [25] have been omitted.

tains trans-membrane insulin receptors, which are kinases. Docking of insulin to the outside causes phosphorylation of tyrosine at the inner side (Fig. 4b). This phosphorylation initiates a signal transduction cascade which finally leads to glucose transport into the cells by a cell-membrane glucose carrier. For details of the signal cascade see, e.g. ref. [25]. In the absence of insulin, or in the case of insulin resistance, the phosphoester bond is hydrolyzed, catalyzed by PTP (c in Fig. 4). In the presence of a vanadium compound, the action of PTP may be counteracted. Vanadate can enter the cell through anion channels; more complex vanadium compounds may overcome the cell membrane either by passive diffusion, if the periphery of the complex is designed so as to allow interaction with the lipid double layer, or via a receptor system, if the complex periphery contains a feature recognizable by a receptor. The possible actions of vanadium are depicted in Fig. 4d–f. Inhibition of PTP by linkage to vanadium (d) has been shown to be a possible mechanism [26]. The phosphoester bond, which also forms by autophosphorylation, thus remains intact and so does the signal transduction pathway. Alternatively, a non-membrane protein–tyrosine kinase (PTK) may be activated by vanadium [27,28] (e). Finally, vanadylation of the receptor tyrosine (f) appears to be a feasible key step in view of the fact that vanadate has substantial affinity to phenol [29] and tyrosine [30]. It has been shown, however, that peroxovanadium compounds do not bind to the receptor [26,31]. The inferences of vanadium compounds depicted in Fig. 4 thus represent only one way of possible action.

Vanadium compounds subjected to in vitro toxicity and insulin-mimetic tests in the context of this report are listed in Scheme 2. Details of related tests carried out in the frame of a European network have been described elsewhere [21]. The compounds, the results of which are presented here, all resemble the active center of the vanadate-dependent peroxidases (Fig. 1) in that their coordination sphere is dominated by oxygen functions, one or two of which are oxo or peroxo groups, and additionally contains a nitrogen function. For comparison, we have included results on the established insulin-mimetic compounds vanadate ($H_2VO_4^-$ under physiological conditions), **3** and $[VO_2(\text{dipicolinate})]^-$ (as the ammonium salt), **9**. Cell toxicity tests have been carried out with simian virus modified mice fibroblasts (cell line SV3T3), insulin-mimetic tests with the same cell line and also with human fibroblasts (cell line F26). In this specific context, insulin-mimesis refers to the ability of

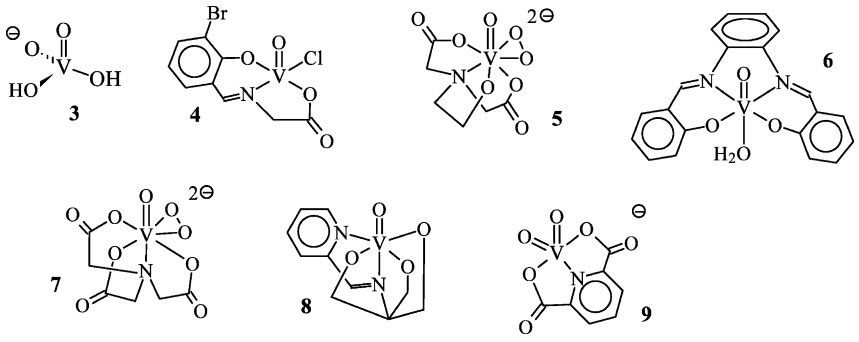

Scheme 2.

the vanadium compounds to trigger glucose uptake with subsequent glucose degradation by cells. The results are presented in Fig. 5.

Practically all of the compounds are toxic at concentrations $c(V) = 1$ and 0.1 mM, while they are non toxic at $c(V) = 0.01$ M and below. There is no obvious increase of the toxic effect as time elapses. In contrast, for compounds **7** and **8**, toxicity decreases with increasing time, possibly as a consequence of cell recovery or adaption. As far as the insulin-mimetic behavior is concerned, there are striking differences for the two cell lines: While, in the case of mice fibroblasts (cell line SV3T3), all of the compounds are significantly less effective than insulin and—with the exception of **3** and **4**—hardly improve the situation encountered with the control group (neither vanadate nor insulin), all of the vanadium complexes are as good as or even more effective than insulin in human fibroblasts. An exception is compound **9** ($[VO_2(dipicolinate)]^-$), which has been found to have insulin-mimetic potency in diabetic cats. These results apparently indicate that (i) in vitro tests cannot unambiguously be used to predict the efficacy in vivo, (ii) the type of cells employed in in vitro tests has to be taken into account (note also that **3** and **4** are among the least effective in human cells), and (iii) low toxicity does not necessarily correlate with high efficacy, as demonstrated by compound **9**, and vice versa, as demonstrated by the peroxo complex **5**, which is one of the more toxic ones but very potent in human fibroblasts. Certainly, these results are not surprising since different cell types exhibit different metabolisms, and the in vivo efficacy also depends on the degree of gastrointestinal uptake, transport capability and stability prior to and during resorption and transport.

3. Experimental

3.1. Materials and instrumentation

1,1-Dichloroethane was distilled over CaH_2 and stored under nitrogen over molecular sieve. 1,2-Dichloroethane was treated with concentrated sulfuric acid (four times with 100 ml of H_2SO_4 per 1 l of dichloroethane), washed with water, dried overnight with $CaCl_2$, distilled over P_2O_5 and stored over molecular sieve. Cumyl-hydroperoxide (Fluka, 80% in cumene) was stored over molecular sieve. $[VO(OiPr)_3]$ (Aldrich), (*R*)-(+)-styrene oxide (Fluka), (*R*)-(+)-1-phenylethylamine (Acros), methyl *p*-tolyl sulfide (Aldrich), benzophenone (Carlo Erba), and bis(*n*-butyl)-sulfide (Aldrich) were used without further purification. An aqueous solution containing vanadates was prepared by dissolving $[NH_4][VO_3]$ in water and adjusting the pH to 7. The following compounds (cf. Scheme 2) were prepared according to literature procedures: **4** [32], **5** [33], **7** [34], **8** [21], **9** [35].

The quantitative product analyses for the catalytically conducted sulfide oxidations were carried out with a Hewlett–Packard 5890 series II chromatograph, equipped with a capillary column with a stationary phase FFAP, EC-1000 (30 m × 0.25 mm, film tickness 0.25 μl). The instrument conditions for the analysis are the following: initial temperature 55 °C for 1 min., rate; 15 °C min^{-1}, final temperature 200 °C for 30 min. The ee for the sulfoxides was determined through HPLC-analysis, using a Shimadzu LC-10AT chromatograph, UV Shimadzu SPD-10A ($\lambda = 241$ nm) detector, and a C-R5A Shimadzu chromatopac integrator. The chromatograph is equipped with a chiral column Chiralcel–Daicel–OD (diameter 0.46, length 25 cm). The eluent employed was a mixture of *n*-hexane–isopropanol 9:1; conditions: flow = 0.6 ml min^{-1}, pressure = 17 kg m^{-2}. The retention time of the *R* enantiomer is 16.2 min, for the *S* enantiomer 18.7 min.

IR spectra were obtained in KBr pellets on a Perkin–Elmer FT 1720, NMR spectra on a Bruker AM 360 or Varian Gemini 200 instrument with the usual spectrometer settings. ^{51}V-NMR chemical shifts are referenced against $VOCl_3$. The X-ray structure analysis was carried out using Mo–K_α irradiation ($\lambda = 0.71073$ Å) on a Smart Apex CCD diffractometer. Hydrogen atoms were calculated into idealized positions and included in the last cycles of refinement. For crystal data and structure refinement see Table 2; for data deposition see CCDC.

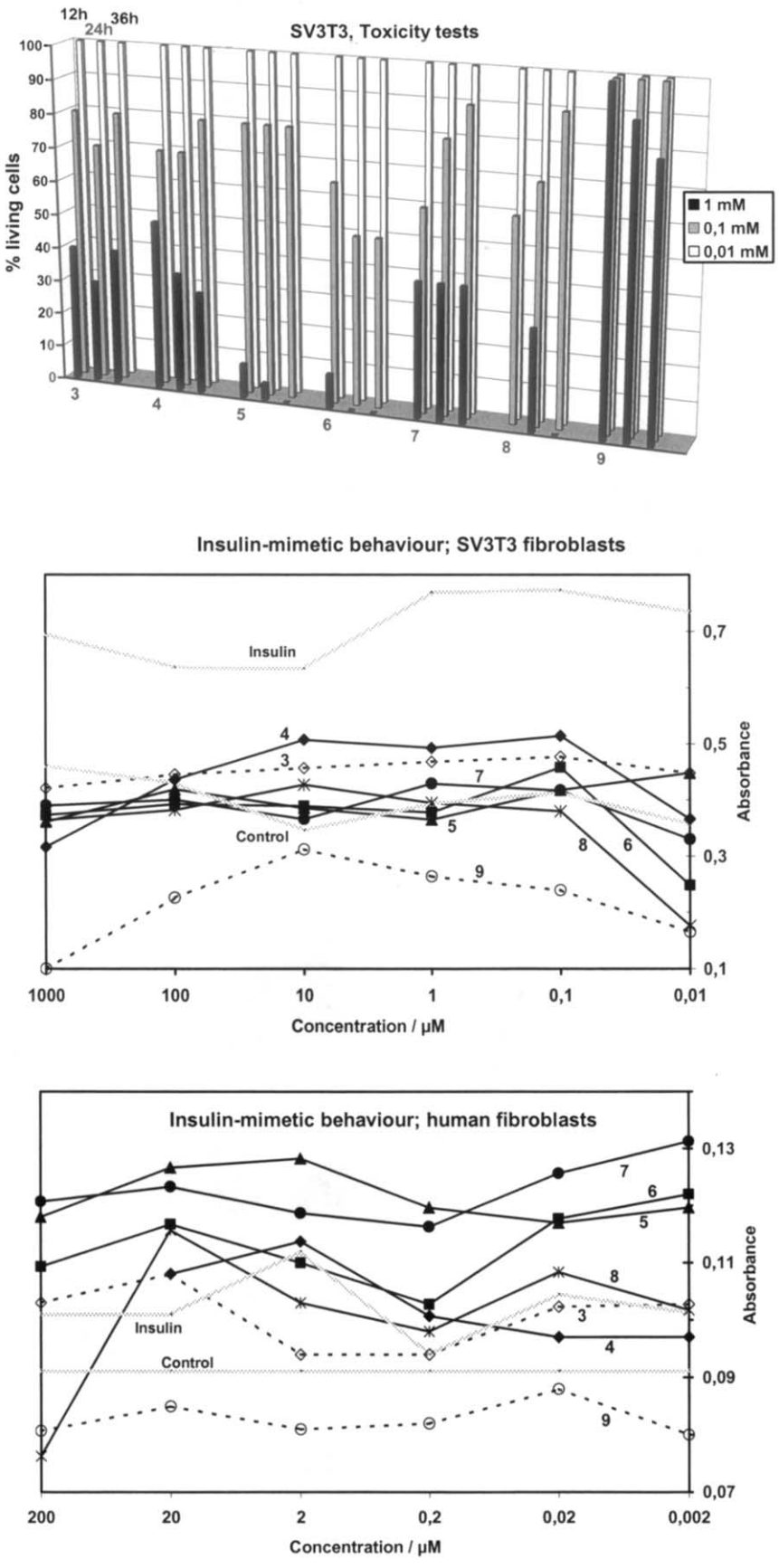
12h
24h
36h
SV3T3, Toxicity tests
% living cells
100
90
80
70
60
50
40
30
20
10
0
3
4
5
6
7
8
9
1 mM
0,1 mM
0,01 mM
Insulin-mimetic behaviour; SV3T3 fibroblasts
Insulin
Control
Absorbance
0,7
0,5
0,3
0,1
1000
100
10
1
0,1
0,01
Concentration / µM
Insulin-mimetic behaviour; human fibroblasts
Insulin
Control
Absorbance
0,13
0,11
0,09
0,07
200
20
2
0,2
0,02
0,002
Concentration / µM

Fig. 5.

3.2. Methods

3.2.1. General procedure for the catalytically conducted sulfide oxidations

In a 1 ml flask, 15.48 mg (0.11 mmol) of methyl-*p*-tolyl-sulfide, 5.12 mg (0.01 mmol) of the vanadium catalyst, and 12.75 mg (0.07 mmol) of the internal standard benzophenone were dissolved in anhydrous 1,2-dichloromethane. The solution was then cooled to 0 °C. Under stirring and in a nitrogen atmosphere, 20 μl (0.011 mmol) of cumyl-hydroperoxide were added. After defined intervals of time, 50 μl portions were removed from the reaction mixture, immediately quenched by adding to an excess of bis(*n*-butyl)-sulfide, and the product spectrum analyzed by GC and HPLC (determination of the ee).

3.2.2. Biological tests

Tests were performed on Simian virus transformed Swiss 3T3 mice fibroblasts (cell line SV3T3), and on human skin fibroblasts of a healthy donor (F26). The fibroblasts were maintained in monolayer cultures at 37 °C under humidified atmosphere containing 5% CO_2. Dulbecco's modification of Eagle's medium (DMEM, Sigma) was employed as the culture medium. The vanadium complexes were applied as solutions in the following solvents: **3** (H_2O), **4** (EtOH), **5** (H_2O), **6** (DMSO), **7** (H_2O), **8** (DMSO), **9** (EtOH). Water solutions were filtered for sterilization.

For toxicity tests, cells were grown to sub-confluency, and the cells were incubated with the vanadium complexes (concentration range 1 mM–10 nM; results for $c(V) < 10$ μM not shown) for 12, 24 and 36 h in DMEM. The cells were treated with trypan blue (0.2% w/v) in phosphate buffered saline solution, and the ratio of stained (living) to non-stained (dead) cells was determined after 5 min of incubation time. The counts were related to the overall amount of cells present (= 100%). Mean error ca. 10%.

Vitality tests for insulin-mimetic activity were based on the MTT-reduction essay. For details, see ref. [21]. Cells were grown to sub-confluency. The medium was then exchanged for serum-free DMEM, supplemented with selenium (5 μg l^{-1}), glucose (3.5 g l^{-1}), transferrin (5 mg l^{-1}), hydrocortisone (0.4 mg l^{-1}), glutamine (200 mg l^{-1}), streptomycin (50 μg l^{-1}) and 50 units of penicillin per ml (all Sigma grade chemicals). The cells were incubated in this (insulin-free) medium for 24 and 72 h, supplemented with MTT (0.5 g l^{-1}), and treated with the solution of the vanadate complexes in the concentration range 1 mM–10 nM (SV3T3) or 0.2 mM–2 nM (F26). After 4 h of incubation, the reaction was stopped with 0.5 M HCl in isopropanol, the dye extracted with isopropanol and the extracts subjected to the photometric measurements. Mean errors for the absorbances are around 0.005 (0.001–0.012).

3.3. Preparation of compounds

3.3.1. (PhMeCH)N(CH_2CHPhOH)$_2$, (*R*,*R*)-bis(2-phenylethanol)-(*R*)-1-phenylethylamine (**1**)

In a 10 ml round bottom flask were placed 5.0 g (41.61 mmol) of (*R*)-(+)-styrene oxide and 2.5 g (20.80 mmol) of (*R*)-(+)-phenylethylamine. The reaction mixture was stirred at 50 °C for 4 days. The crude product thus obtained was purified through flash chromatography on silica gel 60 (Mecherey–Nagel, 230–400 mesh ASTM), using hexane–ethylacetate 8:2 as eluent. The product was obtained as a colorless oil. Yield 5.80 g (82%). Analysis calcd. for $C_{24}H_{27}NO_2$ ($M = 361.48$ g mol^{-1}) C, 79.74; H, 7.53; N, 3.87. Found: C, 79.68; H, 7.61; N, 3.51%. ^{1}H-NMR ($CDCl_3$) δ (mutiplicity, *J* (Hz); number of protons, assignment): 7.33–7.23 (m; 15H, aromatic); 4.63–4.59 (dd, 3.7 and 9.4; 2H, CH_2–**C**HPh–OH); 4.09–4.04 (q, 6.9; 1H, N–**C**HPh–CH_3); 3.80 (bs; 2H, CHPh–**OH**); 2.74–2.64 (m; 4H, N–**C**$\mathbf{H_2}$–CHPhOH); 1.47–1.45 (d, 6.9; 3H, NCHPh–**C**$\mathbf{H_3}$). ^{13}C-NMR ($CDCl_3$) δ: 142.29, 128.37, 128.08, 127.54, 127.44, 125.82 (aromatic carbons); 71.08 (CH_2–**C**HPh–OH); 60.50 (N–**C**HPhCH_3); 59.56 (N–**C**H_2–CHPhOH); 17.72 (NCHPh–**C**H_3). IR (KBr, cm^{-1}): 3368, ν(OH); 3085, 3061, 3027, ν(CH); 2853, ν(NC); 1603, 1585, 1493, 1450, (CC ring stretch); 1092, ν(CO); 755, 700, δ(CH) and δ(CC).

3.3.2. (*R*,*R*,*R*)-[VO(OMe)(O_2N)] · 1/2CH_3OH, **2** · 1/2CH_3OH

In a 2-necked 50 ml round bottom flask, 1.20 g (3.32 mmol) of ligand **1** was dissolved in 20 ml of 1,1-dichloromethane. To this solution, 0.375 g (3.02 mmol) of oxo–tris(isopropoxo)vanadium(V) dissolved in 10 ml of 1,1-dichloromethane was added dropwise. During addition, the color turned to yellow. After 30 min of stirring under nitrogen, the solvent was removed under vacuum. The product was obtained quantitatively as a yellow solid and was recrystallized from methanol. Analysis calcd. for $C_{25.5}H_{30}NO_{4.5}V$ (**2** · 1/2CH_3OH, $M = 473.16$ g mol^{-1}): C, 64.69; H, 6.39; N, 2.96; V, 10.76; found C, 64.78; H, 6.30; N, 2.83; V, 11.02%. ^{51}V-NMR ($CDCl_3$) δ: −414.0, −457.1. IR (KBr, cm^{-1}):

Fig. 5. Toxicity (top) and insulin-mimetic tests for the vanadium compounds shown in Scheme 2. The results for modified mice fibroblasts (center) and human fibroblasts (bottom) include a control group (neither insulin nor vanadium) and a group treated with insulin instead of vanadium. Broken lines correspond to vanadate (**3**) and [VO_2(dipicolinate)]$^-$ (**9**). The ordinate (absorbance) is a measure for the amount of glucose taken up by the cells, as measured by a vitality (MTT) test. Cell toxicity (top) is represented for three concentrations after three periods of time.

3377, ν(OH); 3068, 2966, ν(CH); 2343, ν(NC); 1654, 1601, 1449, (CC ring stretch); 1095, ν(CO); 973, ν(VO) 755, 697, δ(CH) and δ(CC).

*3.3.3. [VO(H$_2$O)(3-Br-sal-gly)] · H$_2$O, **4** · H$_2$O*

The preparation was carried out under N_2. 330 mg (4.40 mmol) of glycine and 1210 mg (8.89 mmol) of sodium acetate trihydrate were dissolved in 30 ml of water and treated dropwise and with stirring with 1030 mg (4.37 mmol) of 3-bromo-5-chloro salicylaldehyde dissolved in 20 ml of ethanol. To this solution, 1110 mg (4.39 mmol) of $VOSO_4 \cdot 5H_2O$ dissolved in 10 ml of water were slowly added. The precipitate which formed during 1 h stirring at room temperature was filtered off, washed twice with 10 ml of a 1:1 mixture of ethanol and water, twice with 10 ml of water, and dried in vacuo. The isolated complex **4** is stable in air. Yield 1.31 g (76%) of light-brown **4** · H_2O. Analysis calcd. for $C_9H_9BrClNO_6V$ ($M = 393.47$ g mol^{-1}) C, 27.47; H, 2.31; N, 3.56; found C, 27.72; H, 2.37; N, 3.57%. IR (KBr, cm^{-1}): 1615, ν(C=N); 1641, $\nu(COO)_{asym}$; 1383, $\nu(COO)_{sym}$; 1003, ν(V=O); 606, $\nu(V-O_{phenol})$. For an XAS characterization, see ref. [36].

4. Conclusion

Vanadate-dependent haloperoxidases contain vanadate(V) covalently linked to a histidine of the protein matrix. They catalyze the two-electron oxidation by peroxide of halide to a halide(+) species, presumably hypohalous acid, but also exhibit oxo transfer activity towards thioethers. If prochiral thioethers are employed, the oxidation to sulfoxides is enantioselective in the case of algal peroxidases. This sulfide peroxidase activity can be modeled by vanadium(V) coordination compounds with vanadium in a coordination environment similar to that found in the native enzymes, viz. (*RRR*)-[VO(L)(OMe)], (**2**), where L^{2-} derives from a trichiral amino-bis(alcohol), **1**. The ee in the non-optimized oxidation of methyl-*p*-tolylsulfide by cumyl-hydroperoxide catalyzed by **2** is 25%. Some sulfoxide is also formed. The same product pattern and ee are obtained with a mixture of **1** and [VO(O*i*Pr)$_3$] as the catalyst system; in this case, however, the reaction is faster by a factor of 5. Other oxidations catalyzed by vanadium compounds have been noted (cf. Bolm et al. in this issue and ref. [37])

The vanadate-free (apo-) peroxidases show phosphatase activity which is lost as the enzymes are reconstituted. This fact conforms with the inhibitory effect of vanadate towards phosphatases. Active site sequence homologies and identical overall structural features have been found between peroxidases (of algal and fungal origin) and acid phosphatase from *E. blattae*. On the other hand, the insulin-mimetic effect of vanadate and vanadium compounds may be traced back to the inhibition of an intracellular protein tyrosine phosphatase by vanadate. Several vanadium compounds, again resembling the active center environment of the peroxidases, have been tested with respect to their ability to trigger glucose uptake by cultured cells from the connecting tissue (fibroblasts) in the absence of insulin. In the case of a human cell line, most of the compounds investigated (**3**–**8**; cf. Scheme 2) are prior to insulin in the concentration range 200–0.002 μM, while they are less effective in modified mice fibroblasts (pseudo-adipocytes). For the modified mice fibroblasts, cytotoxicity has been observed for vanadium concentrations >10 μM. The efficacy of the vanadium compounds discussed here with respect to glucose transport into cells corroborates earlier suggestions to envisage vanadium medication in the oral treatment of diabetes types 1 and 2. It should be kept in mind, however, that the insulin-mimetic potential of vanadium compounds in vivo does not necessarily correlate in a simple manner with in vitro efficacy.

Acknowledgements

This work was supported by the Deutsche Forschungsgemeinschaft, the Fonds der Chemischen Industry, the German Academic Exchange Service, the European Union (COST D12 and COST D21), and the SOCRATES programe.

References

[1] M. Weyand, H.J. Hecht, M. Kieß, M.F. Liaud, H. Vilter, D. Schomburg, J. Mol. Biol. 293 (1999) 595.
[2] M.I. Isupov, A.R. Dalby, A.A. Brindley, Y. Izumi, T. Tanabe, G.N. Murshudov, J.A. Littlechild, J. Mol. Biol. 299 (2000) 1035.
[3] A. Messerschmidt, R. Wever, Proc. Natl. Acad. Sci. USA 93 (1996) 392.
[4] L. Kuchta, M. Sivák, J. Marek, F. Pavelčik, M. Časný, New J. Chem. (1999) 43.
[5] A. Messerschmidt, L. Prade, R. Wever, Biol. Chem. 378 (1997) 309.
[6] M. Casný, D. Rehder, H. Schmidt, H. Vilter, V. Conte, J. Inorg. Biochem. 80 (2000) 157.
[7] M. Casný, D. Rehder, J. Chem. Soc. Chem. Commun. (2001) 921.
[8] (a) H.B. ten Brink, A. Tuynman, H.L. Dekker, W. Hemrika, Y. Izumi, T. Oshiro, H.E. Schoemaker, R. Wever, Inorg. Chem. 37 (1998) 6780;
(b) H.B. ten Brink, H.L. Holland, H.E. Schoemaker, H. van Lingen, R. Wever, Tetrahedron: Asymmetry 10 (1999) 4563.
[9] M.C. Carreño, Chem. Rev. 95 (1995) 1717.
[10] R. Renirie, W. Hemrika, R. Wever, J. Biol. Chem. 275 (2000) 11650.
[11] P.J. Stankiewicz, A.S. Tracey, D.C. Crans, Vanadium and its role in life, in: H. Sigel, A. Sigel (Eds.), Metal Ions in Biological Systems, vol. 31 (Chapter 9), Marcel Dekker, New York, 1995.
[12] K. Ishikawa, Y. Mihara, K. Gondoh, E. Susuki, Y. Asano, EMBO J. 19 (2000) 2412.

[13] (a) D.J. Berrisford, C. Bolm, K.B. Sharpless, Angew. Chem. Int. Ed. Engl. 34 (1995) 1059;
(b) C. Bolm, F. Bienewald, Angew. Chem. Int. Ed. Engl. 34 (1995) 2640;
(c) A.H. Vetter, A. Berkessel, Tetrahedron Lett. 39 (1998) 1741;
(d) C. Bolm, F. Bienewald, Synletter (1998) 13.;
(e) D.A. Cogan, G. Liu, K. Kim, B.J. Ellmon, J. Am. Chem. Soc. 120 (1998) 8011.
[14] W. Adam, D. Golsch, J. Sundermeyer, G. Wahl, Chem. Ber. 129 (1996) 1177.
[15] K. Nakajima, K. Kojima, M. Kojima, J. Fujita, Bull. Chem. Soc. Jpn. 63 (1990) 2620.
[16] H. Schmidt, M. Bashirpoor, D. Rehder, J. Chem. Soc. Dalton Trans. (1996) 3865.
[17] (a) F. Di Furia, G.M. Licini, G. Modena, R. Motterle, J. Org. Chem. 61 (1996) 5175;
(b) M. Bonchio, G.M. Licini, G. Modena, O. Bortolini, S. Moro, W.A. Nugent, J. Am. Chem. Soc. 121 (1999) 6258.
[18] M. Bonchio, G.M. Licini, F. Di Furia, G. Modena, W.A. Nugent, J. Org. Chem. 64 (1999) 1326.
[19a] M. Bashirpoor, H. Schmidt, C. Schulzke, D. Rehder, Chem. Ber./Recueil 130 (1997) 651.
[19b] C. Weidemann, W. Priebsch, D. Rehder, Chem. Ber. 122 (1989) 235.
[20] M.A. Andersson, S.G. Allenmark, Tetrahedron 54 (1998) 15293.
[21] D. Rehder, J. Costa Pessoa, C.F.G.C. Geraldes, M.M.C.A. Castro, T. Kabanos, T. Kiss, B. Meier, G. Micera, L. Pettersson, M. Rangel, A. Salifoglou, I. Turel, D. Wang, J. Biol. Inorg. Chem. 7 (2002) 384.
[22] K.H. Thompson, J.H. McNeill, C. Orvig, Chem. Rev. 99 (1999) 2561.
[23] Y. Sun, B.R. James, S.J. Rettig, C. Orvig, Inorg. Chem. 35 (1996) 1667.
[24] D.C. Crans, J. Inorg. Biochem. 80 (2000) 123.
[25] Y. Zick, Trends Cell Biol. 11 (2001) 437.
[26] B.I. Posner, R. Faure, J.W. Burgess, A.P. Bevan, D. Lachance, G. Zhang-Sun, I.G. Fantus, J.B. Ng, D.A. Hall, B. Soo Lum, A. Shaver, J. Biol. Chem. 269 (1994) 4596.
[27] A. Shisheva, Y. Shechter, J. Biol. Chem. 268 (1993) 6463.
[28] G. Elberg, Z. He, J. Li, N. Sekar, Y. Shechter, Diabetes 46 (1997) 1684.
[29] B. Galeffi, A.S. Tracey, Can. J. Chem. 66 (1988) 2565.
[30] A. Tracey, M.J. Gresser, Proc. Natl. Akad. Sci. USA 83 (1986) 609.
[31] I.G. Fantus, S. Kadota, G. Deragon, B. Foster, E.I. Poster, Biochemistry 28 (1989) 8864.
[32] X. Wang, X.M. Zhang, H.X. Liu, Transition Met. Chem. 19 (1994) 611.
[33] C. Dordjevic, P.L. Wilkins, E. Sinn, R.J. Butcher, Inorg. Chim. Acta 230 (1995) 241.
[34] G.J. Colpas, B.J. Hamstra, J.W. Kampf, V.L. Pecoraro, J. Am. Chem. Soc. 116 (1994) 3627 and 3469.
[35] K. Wieghardt, Inorg. Chem. 17 (1978) 57.
[36] H. Dau, J. Dittmer, M. Epple, J. Hanss, E. Kiss, D. Rehder, C. Schulzke, H. Vilter, FEBS Lett. 457 (1999) 237.
[37] T. Hirao, Chem. Rev. 97 (1997) 2707.